Extended Abstracts of the 2010 International Conference on Solid State Devices and Materials, Tokyo, 2010, pp11-12

Carrier Propagation Dependence on Applied Potentials in Pentacene OFET Investigated by Impedance Spectroscopy and Electrical Time-of-Flight Techniques

Jack Lin[1], Martin Weis[2], Dai Taguchi[1], Takaaki Manaka[1] and Mitsumasa Iwamoto[1]

[1] Department of Physical Electronics, Graduate School of Science and Engineering,
Tokyo Institute of Technology,
2-12-1 O-okayama, Meguro-ku, Tokyo 152-8552, Japan
Phone: +81-3-5734-2191 E-mail: iwamoto@pe.titech.ac.jp
[2] Institute of Physics, Slovak Academy of Sciences
Dúbravská cesta 9, 845 11 Bratislava 45, Slovak Republic

1. Introduction

Organic semiconductors have shown great potential in various application, such as organic photovoltaic cells (OPVC), organic field effect transistors (OFET) and organic light emitting diodes (OLED). Among these potential applications, OFET can be used to make flexible circuitry. In conjunction with other applications of organic semiconductors, flexible displays or solar cells have already been successfully demonstrated. Additionally, organic radio frequency identification (RFID) also sees a large market that has been forecasted to overtake the display market in the near future.

Previously, we have reported the technique for evaluation of transit time by the phase response in impedance spectroscopy (IS) and electrical time-of-flight (TOF) techniques. In IS, the device is subjected to a small-signal alternating current (AC) perturbation across a wide range of frequencies. The transit time evaluation method is based on the carrier propagation across the channel region of an OFET, and observing the critical frequency where the phase begins to drop, signifying the successful transit of carriers across the channel. The electrical TOF technique uses the delay between the applied boxcar voltage and drain current for determination of the transit time.

In this report, we further apply these techniques to show the dependence of carrier propagation on the applied potentials, including gate-source potential (V_{gs}) and drain-source potential (V_{ds}), and also the charging effect of the device.

2. Experimental

Top-contact pentacene OFETs were prepared for the experiments (the sample structure is shown in Figure 1). Heavily-doped Si wafers with a 100 nm thick thermally prepared silicon dioxide (SiO_2) insulating layer were used as the base substrates. The substrates were ultrasonically cleaned by acetone, ethanol, and water, and then UV/ozone cleaned for 30 minutes before deposition of the organic layer. The pentacene deposition was carried out below 2×10^{-6} Torr and the deposition rate was kept at 0.5 Å/s, monitored by a quartz crystal microbalance. The pentacene was purchased from Tokyo Chemical Industry Co., Ltd., and was used without further purification. Au-electrodes of 50 nm in thickness were deposited on the pentacene surface below 4×10^{-6} Torr. The channel width and lengths (W and L) were 3 mm and 30 to 100 μm, respectively. The OFETs were investigated by standard current-voltage (I-V) analysis using Keithley 2400 SourceMeter, as well as impedance spectroscopy using Solartron 1260 impedance/gain-phase analyzer. Here in the IS measurement, the amplitude of the AC signal was 0.5 V superposed on various DC biases up to 40 V_{ds}. In the electrical TOF measurement, the boxcar voltage is generated by the function generator NF WF1974 and amplified by the high-speed amplifier NF BA4825. The current is obtained by the potential drop across a load resistor (10 kΩ) connected to the drain electrode, monitored by the oscilloscope Tektronics DPO3014.

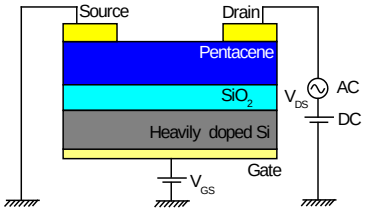

Figure 1 Schematic of the sample

3. Results and discussion

The I-V measurement shows typical output and transfer characteristics of an OFET, with a threshold voltage of about 5 V and mobility about 0.04 cm^2/Vs.

Our previous report [1] has shown that the two relaxation processes observed in this experimental setup are attributable to the injection and transport properties of OFET. The impedance phase response shows that the critical frequency where the phase begins to drop moves to a higher frequency systematically with increasing applied gate bias (Figure 2). This experimental result suggests that the transit time becomes shorter (or mobility is higher) for higher applied gate bias. From these results, the critical frequency f can be used to calculate the transit time t_{tr} by $t_{tr} = 1/2f$.

The electrical TOF technique also shows similar trend of voltage dependence. This technique gives us a more direct indicator of the transit time by the delay of current rise in comparison to the applied boxcar voltage. Both impedance spectroscopy and time-of-flight techniques were tested across different voltages and channels (Figure 3). The change of steady-state current in TOF corresponds well

with conventional current-voltage measurement.

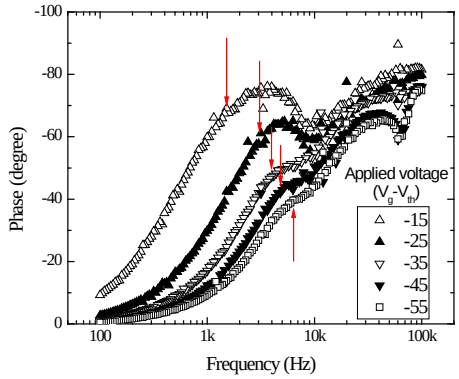

Figure 2 Phase response at various gate biases (V_{ds} = -3 V)

From the standard drain-source current equation in the linear region,

$$I_{ds} = C_g \frac{W}{L} \mu \left(V_{gs} - V_{th} - \frac{1}{2} V_{ds} \right) V_{ds} \qquad (1)$$

where C_g and μ are the gate insulator capacitance and mobility, the differential channel resistance can be estimated. Hence, the average relaxation time (*RC*) represents the transit time for carriers to cross the channel, and is obtained by the following proposed expression similar to that of the conventional time-of-flight method:

$$t_{tr} = \frac{1}{2\left[\left(V_{gs} - V_{th}\right) - V_{ds}\right]} \frac{L^2}{\mu}. \qquad (2)$$

This corresponds to the abovementioned dependences of the transit time on gate and drain biases. The shift of the critical frequency in IS experiments also agrees well with this relationship.

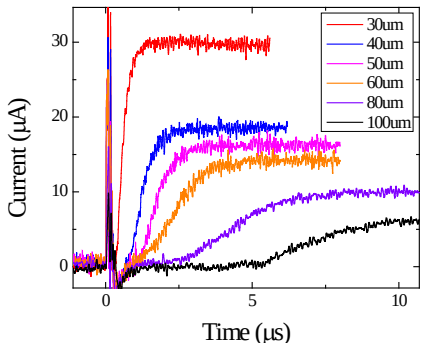

Figure 3 TOF response across various channel lengths

To further verify this relation, the transit time was plotted as a function of the square of channel length. A linear relation can be found (Figure 4). However, notice that the extrapolation of this relation leads to a non-zero intercept, which can be attributed to the charging time of the device prior to transport. The charging time was estimated to be ~0.1 ms, which also relates to the contact resistance R_C by the $R_C.C_g$ relation.

As a result, transit time mentioned previously includes the charging time and transport time, which reflects the carrier mobility. Hence, we obtain a strong tool to evaluate the transient mobility in OFETs. The mobility estimated by this method is ~0.02 cm^2/Vs. This value is slightly smaller than the mobility estimated by I-V (~0.04 cm^2/Vs). The discrepancy dwells in the transient mode of the measurement where the trapping effect slows down the carrier transport, in comparison with the steady-state measurement where traps are filled. By comparison of the transient and steady-state mobility, it is possible to estimate the time that carriers spend in traps. For the 30 μm channel, it is estimated to be about 5 μs, which is comparable to the transport time.

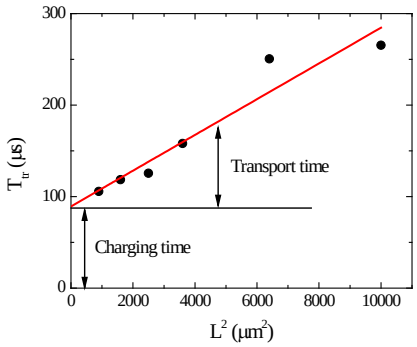

Figure 4 Dependence of the transit time to L^2

4. Conclusions

Impedance spectroscopy and electrical TOF techniques were applied on the OFET structure to characterize the carrier's dependence on applied voltages. This method is based on carrier propagation, thus filters out possible contributions from changes in charge density. We found that as the gate bias increases, transit time is reduced.

Our proposed model explains these experimental results, and allows us to evaluate the transient mobility. The linear relation between transit time and square of the channel length supports this model. Additionally, the charging time of OFET was found, and can be used for evaluation of contact resistance R_C by the $R_C.C_g$ relation. This approach can be used for characterizing various parameters of OFET in the transient state, and was used for improving the standard model. It is significant for potential applications of organic electronic devices which will operate in the transient state, such as RFID.

Acknowledgements

This work is support by the Grants-in-Aid for Scientific Research (Grant 20656052 and Priority A 19206034) from Japan Society for the Promotion of Science (JSPS)

References

[1] J. Lin, M. Weis, D. Taguchi, T. Manaka and M. Iwamoto, Thin Solid Films 518, 448 (2009).

[2] D. Basu, L. Wang, L. Dunn, B. Yoo, S. Nadkami, A. Dodabalapur, M. Heeney, I. McCulloch, Appl. Phys. Lett. 89, 242104 (2006).